The Journal of Neuroscience, July 1994, 14(7): 4147–4158

Activity-Dependent Expression and Distribution of M_1 Muscarinic ACh Receptors in Visual Cortex Neuronal Cultures

Yihong Wang,[1] Qiang Gu,[1] Fei Mao,[2] Richard P. Haugland,[2] and Max S. Cynader[1]

[1]Department of Ophthalmology, University of British Columbia, Vancouver, British Columbia, Canada V5Z 3N9 and [2]Molecular Probes Inc., Eugene, Oregon 97402

The fluorescently labeled muscarinic M_1 receptor–selective antagonist BODIPY® FL pirenzepine has been employed to study the activity-dependent distribution and expression of muscarinic M_1 ACh receptors (M_1AChRs) in cultured neurons derived from rat visual cortex. Displacement experiments showed that like pirenzepine, binding of BODIPY® FL pirenzepine was specific to M_1 receptors and its K_i was similar to that of unlabeled pirenzepine. Using confocal laser scanning microscopy, M_1 receptors were predominantly localized to cell bodies early in development in the culture environment. After 2 weeks in culture, the receptors showed labeling not only in cell bodies but also in neuritic processes, especially on the initial segments of the processes. Chronic membrane depolarization with 40 mM potassium chloride caused a dramatic increase in M_1 receptor expression on these neurons. Conversely, blockade of neural activity with 0.1 μM TTX decreased expression of the receptors. Receptor expression increased after cells were treated chronically with 50 nM pirenzepine, whereas it decreased after exposure to 10 μM carbachol. The results demonstrate for the first time the exact location of muscarinic receptors in living cultured neurons and also the activity-dependent expression of M_1 receptors on these neurons. Both chronic membrane depolarization and antagonist application upregulate receptor expression, whereas blocking bioelectrical activity or chronic agonist application downregulates expression.

[Key words: visual cortex, cultured neuron, muscarinic M_1 receptor, ACh, BODIPY® FL pirenzepine, carbachol, atropine, nicotine, receptor expression, receptor distribution, confocal microscopy, bioelectric activity, TTX]

Acetylcholine (ACh) is a major excitatory transmitter in the mammalian CNS. In visual system, ACh has been found to be associated with the nonspecific effects of arousal in the cortex (Singer, 1979) and to modulate visual information processing within this structure (Sillito and Kemp, 1983). In addition, cholinergic mechanisms may also play a role in the control of visual plasticity (Bear and Singer, 1986; Gu and Singer, 1993).

The heterogeneous nature of the muscarinic ACh receptors (mAChRs) was discovered a decade ago (Birdsall et al., 1978), and current evidence indicates that there are at least five different muscarinic receptors (designated M_1, M_2, M_3, M_4, and M_5) (Hulme et al., 1990). The discovery of the selective M_1AChR antagonist pirenzepine (PZ) (Hammer et al., 1980), which has a much higher affinity for M_1AChRs than for the other mAChRs subclasses, has made it possible to label directly and selectively the M_1 subtype using ^{3}H-PZ as ligand (Watson et al., 1982).

Studies of M_1AChRs have been focused on their location in the CNS, their mechanism of action, their function, and their primary structure. In previous studies from our laboratory, we have studied the pattern of developmental expression and distribution of this receptor type in cat visual cortex (Cynader et al., 1990; Prusky and Cynader, 1990) using ^{3}H-PZ for receptor autoradiography. We found substantial changes in M_1 receptor distribution and density during postnatal development, with different cortical layers showing markedly different concentration of receptors at different ages. Moreover, this developmental redistribution of M_1AChR could be modulated by the nature of input to the cortex during early development. In addition, we have studied regulatory mechanisms of mAChRs in short-term living slices of rat cerebral cortex (Jia et al., 1989; Shaw, 1989; Van Huizen et al., 1989). However, despite these studies there is still much to learn about the use and activity dependency of these receptors in living neurons. Most studies of M_1 receptors that we and others have performed have utilized two techniques, autoradiography and immunocytochemistry. These have revealed that the M_1 receptor is prevalent in sympathetic ganglia (Brown et al., 1980; Giraldo et al., 1985) and in brain areas such as cerebral cortex, corpus striatum, and hippocampus (Mash and Potter, 1986; Spencer et al., 1986; Prusky and Cynader, 1990). While we have provided evidence of redistribution of receptors with age, these studies still provide only static views of receptor distribution in fixed tissues.

A new optical microscopic technique, confocal laser scanning microscopy, offers significant advantages over conventional epifluorescence microscopy, including the possibility of a significant improvement in lateral resolution and the capability for direct noninvasive serial optical sectioning of intact and even living specimens (Shotton, 1989; Pawley, 1991). Using this new technique for visualization of neurotransmitters and/or their receptors in living neurons may lead to a greater understanding of their roles in the functioning brain. Recently this technique has been used to study GABA and glutamate interactions in rat cortex (Vincent et al., 1991) and to examine glycine synaptic receptors in goldfish brain slices (Triller et al., 1991).

It has now been established that long-term variations in neural activity can alter the normal development of synapse number

Received July 1, 1993; revised Dec. 15, 1993; accepted Dec. 31, 1993.

This work was supported by MRC Program Grant PG-29 to M.S.C. and the Network of Centers of Excellence for Neural Regeneration and Functional Recovery.

Correspondence should be addressed to Dr. Yihong Wang, Department of Ophthalmology, University of British Columbia, 2550 Willow Street, Vancouver, B.C., Canada V5Z 3N9.

and structure in the cortices of experimental animals (Van Huizen et al., 1985, 1987; Beaulieu and Cynader, 1990a,b). Studies of mAChRs also show that the receptor up- and downregulation is induced by multiple factors including physiological, pharmacological, and pathological changes (Maloteaux et al., 1983; El-Fakahany and Lee, 1986; Hunter and Nathanson, 1986; Pedigo, 1988; Pilch and Muller, 1988; Zhu and Chuang, 1988; Rimvall et al., 1989; Thompson and Ficher, 1990; Bhattacharya et al., 1991). We have examined these questions for M_1 receptors in living cortical cells in primary culture, asking how readily receptor number and distribution can be altered and what role receptor input and neuronal activity play in the process. In order to address above questions, we have established a model system using fluorescent PZ to visualize M_1 receptors directly by confocal microscopy in cultured neurons derived from rat visual cortex.

Materials and Methods

Rat brain dissection and primary cell culture preparation. Visual cortex neuronal cells in culture were prepared from postnatal day 0 or day 1 Long-Evans rats. Each rat was killed by decapitation under halothane anesthesia. The cerebral hemispheres were removed and placed in a 60 mm culture dish with brain dissecting buffer solution containing Ca^{2+} and Mg^{2+} free Hank's Balanced Salt Solution (GIBCO) of the following composition (in mM): NaCl, 138; KCl, 15.7; KH_2PO_4, 0.3; Na_2HPO_4, 0.3; dextrose, 18; $NaHCO_3$, 4; HEPES, 15.7 (Sigma); pH 7.4. Under a dissecting light microscope, the visual cortices were dissected and minced with iridectomy scissors into fine fragments. The fragments were then transferred into a 15 ml centrifuge tube containing 2 ml of 0.25% trypsin (Sigma) and 1 ml of 0.1% DNase I (Boehringer Mannheim). The tissue was incubated in a 37°C incubator for 10 min, and then removed and gently dissociated with a 5 ml plastic pipette; 2 ml of ice cold fetal bovine serum was added to the cell suspension to stop the trypsin activity. The cell suspension was then centrifuged, and resuspended in culture medium (Minimum Essential Medium, MEM; GIBCO) containing (in mM) L-glutamine, 4; $NaHCO_3$, 16; HEPES, 20; and 10 ml of fetal bovine serum; pH 7.4. After two washes with fresh medium, the cells (10^6 cells per ml) were plated onto poly-L-lysine–pretreated glass coverslips (described below) in 35 mm culture dishes. Each culture dish contained 2 ml of culture medium. The cultures were incubated in a 5% CO_2 incubator at 37°C. The medium was totally removed on the following day and replaced with fresh medium containing 20 μM cytosine arabinofuranoside (Sigma) to limit the proliferation of glial cells (Greene and Rein, 1976). Half of the medium was then replaced at twice weekly intervals with fresh medium without cytosine arabinofuranoside.

Coverslip preparation. Thirty-one millimeter circular glass coverslips (Biophysica Technologies, Inc.) were boiled in 50% nitric acid for 2 hr and rinsed with running tub water and then distilled water for at least 20 min. The coverslips were transferred into glass petri dishes for sterilizing in an autoclave at 125°C for 25 min, and then placed in an autoclave drying oven (60°C) overnight. Each coverslip was plated into a 35 mm culture dish before the rat brain dissection; 0.5 ml of poly-L-lysine solution (P-L-L; 0.1 mg/ml in distilled water; Sigma) was dropped onto each coverslip to cover the glass surface. The P-L-L solution was left on for about 20–30 min, and then aspirated away, and the coverslip was rinsed three times with sterile water.

Cell culture conditions. Cultures were incubated in the MEM medium described above for 10 d before the treatments described below were applied. For study of activity-dependent and use-dependent receptor expression, cell cultures were then divided into several groups that were incubated in MEM containing either (1) 40 mM potassium chloride, (2) 0.1 μM tetrodotoxin (TTX; Sigma), (3) 5 nM unlabeled PZ (Research Biochemicals Inc., RBI), or (4) 10 μM carbachol (RBI), respectively. The media were also changed at twice weekly intervals. After 7 d of incubation in the above media, the cultures were ready to be examined.

Synthesis of BODIPY® FL PZ. The M_1-selective muscarinic receptor antagonist pirenzepine (5,11-dihydro-11-[[4-[2-[6-(t-Boc-amino)-1-oxohexyl]-amino]ethyl]-1-piperazinyl]-6H-pyrido[2,3-b][1,4]benzodiazepin-6-one) was synthesized according to the reported procedure (Karton et al., 1991), except that 6-tBoc-aminohexanal, which was also required for the synthesis, was made using the method of Martinez (Martinez et al., 1985). Trifluoroacetic acid (TFA; 0.5 ml) was added dropwise to the above intermediate (60 mg, 0.11 mmol) in 3 ml of $CHCl_3$ cooled in an ice bath. After the addition, the solution was warmed to room temperature and stirred overnight. The solvent and excess TFA were rotor evaporated, and the gummy residue was further dried under high vacuum for 2 hr to remove the remaining TFA. The residue was then suspended in 15 ml of dry $CHCl_3$, followed by the addition of diisopropylethylamine (100 μl). 4,4-Difluoro-5,7-dimethyl-4-bora-3a,4a-diaza-s-indacene-3-propionic acid, succinimidyl ester (NHS BODIPY; 43 mg, 0.11 mmol) in 15 ml of dry $CHCl_3$ was added dropwise to the above stirred suspension, and the stirring continued overnight at room temperature. The solvent was removed by rotor evaporation. The product was isolated by the preparative TLC using MeOH/$CHCl_3$ (1:4) ($R_f = 0.5$) as the solvent. The product was identified by NMR and high-resolution mass spectroscopy.

BODIPY® FL PZ binding procedures. Cells were incubated in total darkness for 60 min at room temperature with 50 nM BODIPY® FL PZ in HEPES-buffered saline containing (in mM) 138 NaCl, 5 KCl, 0.8 $Na_2HPO_4 \cdot 2H_2O$, 10 $MgSO_4$, and 20 HEPES, pH 7.4. Time course studied indicated that after about 50 min of incubation, the maximum fluorescent intensity appeared to reach asymptote (Fig. 1). Therefore, we chose a 60 min incubation time for our studies. At the end of the incubation period, the cells were rapidly washed twice with HEPES buffer. Displacement experiments to evaluate binding specificity were performed by incubating BODIPY® FL PZ (50 nM) in the presence of other muscarinic receptor antagonists including unlabeled PZ, AF-DX 116 (Boehringer Ingelheim Ltd., Canada), 4-DAMP methiolide (RBI), and atropine (Sigma). For those cultures that had been pretreated with unlabeled PZ and carbachol, an extra rinsing step was applied to wash off the drugs from receptor binding sites before BODIPY® FL PZ binding was undertaken.

Evaluation of BODIPY® FL PZ affinity by radioligand binding assay. The binding assays were conducted on homogenates of rat cortex membranes as described in other studies (Araujo et al., 1991). Male Long-Evans rats (250 gm) were decapitated under halothane anesthesia and the brains were dissected on ice. Both brain hemispheres were homogenized with a Brinkmann Polytron (setting 6, 20 sec) in Krebs' buffer containing the following (in mM) NaCl, 120; $MgSO_4 \cdot 7H_2O$, 1.2; KH_2PO_4, 1.2; glucose, 5.6; $NaHCO_3$, 25; $CaCl_2$, 2.5; and KCl, 4.7; pH 7.4. The homogenate was centrifuged for 10 min at 490,000 × *g*, after which the supernatant was discarded and the pellet washed twice by resuspending in fresh buffer and recentrifuging. The final membrane pellet was suspended in buffer. Aliquots of the final membrane pellet (200–500 μg of protein) were incubated in the same buffer as above, containing 10 nM (*N*-methyl)-^{3}H-PZ (72 Ci/mmol; New England Nuclear, Boston, MA) and various concentrations of competing ligands including BODIPY® FL PZ, PZ, and nicotine (as control) for 60 min at 4°C. Bound ^{3}H-PZ was separated from free ^{3}H-PZ by centrifuging the membrane pellet, discarding the supernatant, and washing twice in fresh buffer as described above. The radioactivity bound was detected with a scintillation counter (Beckman Inc., Fullerton, CA). The data from the radioligand competition binding assays were expressed as percentages of the maximum specific binding of the radioligands observed in the absence of competitor. IC_{50} values were obtained graphically and then corrected for occupancy by the labeled ligand according to the method of Cheng and Prusoff (1973) to obtain K_i values. The K_i values presented are geometric means [anti-log of averaged log (K_i) values].

Confocal microscopy. The incubation steps with BODIPY® FL PZ and washes were performed as described above. The glass coverslips with the cells attached were removed from the culture dishes to a Teflon chamber (Bionique), which provides an optically clear surface for improved microscopic resolution (Gabridge, 1981). This chamber then was placed onto the stage of a confocal microscope.

Cells were initially viewed using a fluorescein isothiocyanate–specific dichroic filter with the epifluorescence optics of a Nikon Microscope DIAPHOT-TMD; 20× fluotar and 60× oil immersion objectives were used to give first overall and then high-magnification views.

Confocal imaging was performed with the MRC-600 laser scanning confocal system (Bio-Rad Microscience) configured with a Nikon microscope, argon ion laser (488/514 nm), and a PC-AT–compatible computer system integrated with an optical disk for image storage. The basic optical design of the laser light pathway has been fully described elsewhere (Carlsson and Aslund, 1987, 1989; Shotton, 1989; Pawley, 1991). All image-generating and processing operations were performed by soft-

ware provided with the confocal system. The optical scanning images (768 × 512 pixels) of visual cortex neurons either were taken from lookthrough projection (with the spatial filter aperture fully opened), or were composited from 10 sections at 1 μm intervals so that a total thickness of 10 μm of each neuron was imaged. From these data volumes, the image of each neuron could be generated and used for evaluation of M_1 receptor localization. The collected images were stored in the memory of the MRC-600 data station for subsequent analysis. This method permitted selection of only those individual optical sections that contained the neuronal elements of interest for construction of a final image and thus provided an apparent extension of depth of field for the objects being analyzed. The imaging process also included contrast enhancement by signal amplification and background noise reduction. In addition, combining two individual images of the same field could produce a single image that yielded a "3-D–like" quality to the image so that the BODIPY labeled binding sites appeared in relief from the background. From this kind of computer-enhanced image, the relative anatomical relationships of the binding sites to cell structures could be observed. Following the use of an on-screen magnification zoom option, high-magnification images of the individual fluorochromes on the receptor binding sites could be visualized on the monitor. Hard copies were then generated by using Kodak Ektachrome slide film (ASA 100) to photograph the monitor.

In order to make reliable quantitative measurement of fluorescent binding sites, the following procedure was applied. First, at low magnification (20× objective) and using phase-contrast condenser, a search field was randomly chosen. Then neurons within this field were examined one after another using a high-power objective (60× oil objective). The distribution and density of fluorescent labeling on each individual neuron were captured with the confocal microscope. The maximum contrast of the image was achieved by adjusting the photomultiplier output. Once the optimal image was obtained, the same level of photomultiplier output was used to capture the rest of the images in the same experiment. The fluorescent clusters were then analyzed on the screen monitor. In this way, photobleaching, associated with data collection (fade), could be reduced to a minimum. The locations of clusters were identified and assigned to groups corresponding to somata and process locations.

Evaluation of binding specificity by confocal microscopy. The binding specificity of BODIPY® FL PZ for the M_1 receptor was determined by confocal imaging in the presence of different antagonists for muscarinic receptors. In these experiments the cultured neurons were incubated concurrently with 5 nM BODIPY® FL PZ and various antagonists for M receptors at concentrations of 5 μM or 50 μM. PZ was used to displace fluorescent labeling of M_1 receptors. AF-DX 116 and 4-DAMP methioide were used to occupy M_2 and M_3 receptors, respectively, and atropine was applied to occupy all classes of muscarinic receptors in a nonselective manner. To evaluate binding density, 10 different frames were captured for each one preparation. The pixel intensity distribution histogram was then plotted for each frame. The intensity value of most strongly fluorescent pixel in each screen was normalized to 100% and then binding intensity in the various conditions described above was compared to this value.

Results

Morphological development of rat visual cortex neurons in primary cell culture as studied by phase-contrast microscopy

The freshly seeded cells adopted a rounded shape without extensions. A few cells began forming small extensions within 1 hr of plating and most cells formed extensions within 8 hr. The extensions differentiated into one long neurite (the probable axon) and several short ones (probable dendrites) per cell within 24 hr. At 24 hr, a few glial cells were seen as large, flattened, phase-dark cells with broad extensions. The cultures developed well during the first 10 d *in vitro* (DIV) without any special treatment. Small bi- and multipolar neurons (presumably nonpyramidal cells) and large neurons that resembled pyramidal cells were present either as solitary elements or as small clusters of cells on patches of flat glial cells by 10 d in culture. The outgrowth of neurites led to a network in the central area of the plate. After another 7 d without treatment the control cultures showed a well-developed neuronal network and a full layer of glial cells (Fig. 2*B*). In high K^+–treated cultures, the number of neuronal cells was the same as that of the control cultures. The size of neuronal cell bodies was also the same or perhaps slightly enlarged. Their processes (especially pyramidal-like neurons) were extensively spread out with enriched varicosities. The neuronal network therefore tended toward a more dense appearance (Fig. 2*A*). In the TTX-treated cultures, the neurons also retained the same size and a slightly reduced number. However, the network of branched neurites was markedly reduced (Fig. 2*C*).

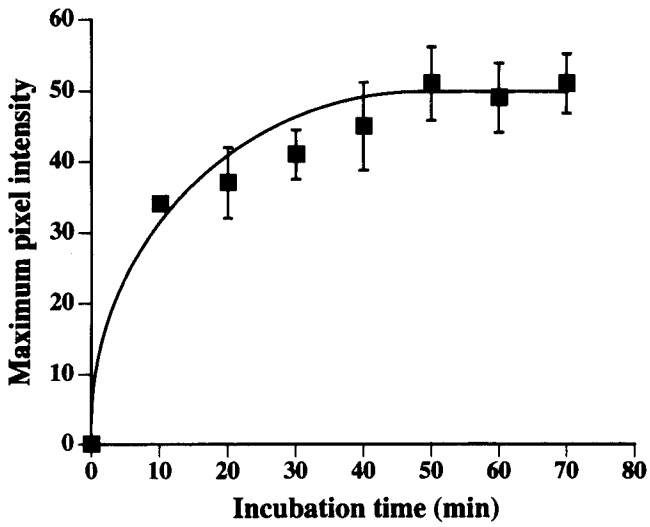

Figure 1. Association time course of BODIPY® FL PZ binding as studied in cultured rat visual cortical neurons. Cultures were exposed to BODIPY® FL PZ for the time indicated and then confocal images were obtained. The maximum pixel intensity measured from each image was used to obtain the data reported for the figure plotting. Values are the means (±SEM) of five experiments. The curve is fitted by eye.

The general morphology of neurons in PZ- and carbachol-treated cultures were also investigated under phase-contrast microscope. No significant changes were found in either the size or density of the neuronal cells or in the appearance of the neuronal network.

After 3 weeks *in vitro,* the control cultures started to show signs of degeneration such as the formation of lipid droplets in the neurons and in other cells, retraction of neurites, and abundance of fine cell debris. For this reason, our experiments were performed on neurons only during the first 3 weeks in culture.

High binding affinity of the BODIPY® FL PZ to its receptor site on the M_1 receptor

The displacement curves (Fig. 3) for BODIPY® FL PZ indicate that this compound retains the high affinity of the parent nonfluorescent compound and that it effectively displaces ^{3}H-PZ binding. The calculated K_i value for BODIPY® FL PZ was 52 nM compared with a K_i for unlabeled PZ of 38 nM, obtained in the same experiment. These results show that derivatization has only a minor effect on the equilibrium binding of PZ to its site on the M_1 receptor.

Visualization of M_1 AChR binding sites in cultured visual cortical neurons

The expression of M_1AChRs was assayed by the binding of BODIPY® FL PZ to living visual cortical neurons in cultures.

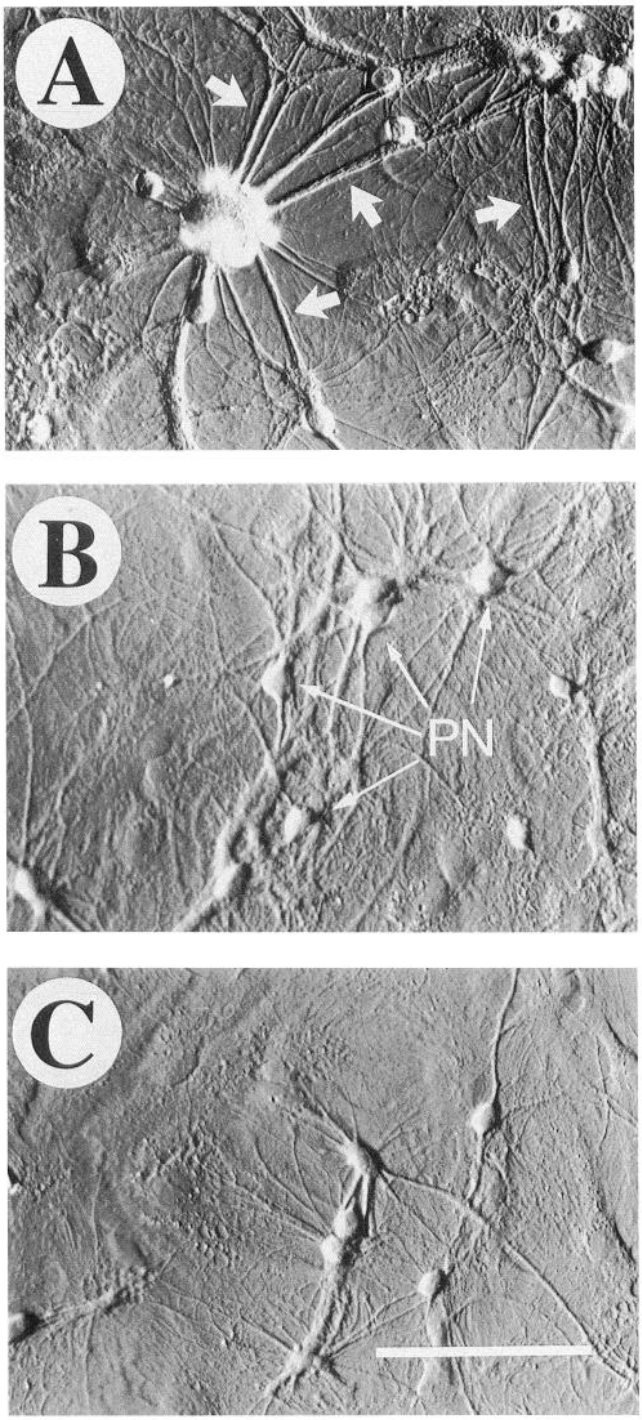

Figure 2. Photographs of a visual cortex neuronal culture taken with a phase-contrast microscope. *A*, A 17-d-old culture that has been exposed to 40 mM K^+ for 7 d shows a thick-appearing neuronal network and enriched varicosities on cell processes (*arrows*). *B*, A control culture of 17-d-old neurons shows pyramidal neurons (*PN, arrows*) and the neuronal network. *C*, A 17-d-old culture that has been exposed to 0.1 μM TTX for 7 d shows a significant reduction of the network of branched neurites. Scale bar, 100 μm.

Figure 4*B* shows a typical confocal image of the distribution of receptor binding sites taken from a pyramidal neuron after 10 d in culture. This image was obtained by projecting and compositing scanning images (768 × 512 pixels) of the neuron at 1 μm intervals for a total of 10 sections. The same extended focus

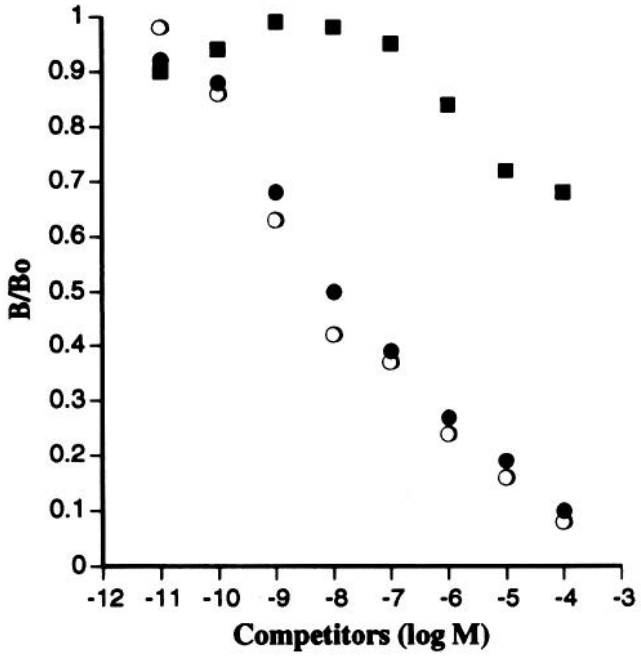

Figure 3. Competition for ^{3}H-PZ binding to the high-affinity sites in rat brain cortex membranes. Experimental details are explained in Materials and Methods. *Bo* and *B* are binding in the absence and in the presence of unlabeled competitor, respectively. Each value represents the mean of three separate experiments. Displacement by PZ (○), BODIPY® FL PZ (●), and nicotine (■) are indicated. *M* is the concentration of competitors. Note that BODIPY® FL PZ and natural PZ are about equally effected displaces while nicotine is much less effected.

method was used to create the other confocal images presented in this article. As shown in Figure 4*B*, receptor binding sites were clearly visualized as fluorescent "hot spots" on the cell body and proximal portions of processes that could not always be followed over long distances. These fluorescent hot spots were circular or roughly oval and were fairly homogeneous in size, with most diameters varying from 0.5 to 1.5 μm.

Specific binding of BODIPY® FL PZ to M_1 receptor

Displacement experiments as described in Materials and Methods were performed in order to determine whether the BODIPY® FL PZ binding to M_1AChR could be displaced by concurrent incubation with various muscarinic antagonists. The results from these experiments are shown in Figure 5. The maximum fluorescent intensity decreased to 7% of control levels for the neurons incubated with 5 nM BODIPY® FL PZ and 5 μM unlabeled PZ to compete for the M_1 receptors. Both 5 μM AF-DX 116 and 5 μM 4-DAMP had little or no effect on the binding of BODIPY® FL PZ to its receptors, with the mean pixel fluorescent intensity maintained at 92% and 89% of control levels, respectively. For those neurons exposed to 5 μM atropine, the binding of BODIPY® FL PZ to the receptor was almost completely blocked as indicated by a drop to only 8% of baseline fluorescence intensity. These results indicate that chemically coupled BODIPY® FL PZ still maintains its high binding affinity and specificity for M_1AChRs.

Developmental expression and distribution of M_1 receptor

The expression and distribution of M_1 receptors were studied after different lengths of time in culture. As shown in Figure 6*A*, receptors were already expressed on the cell bodies of neu-

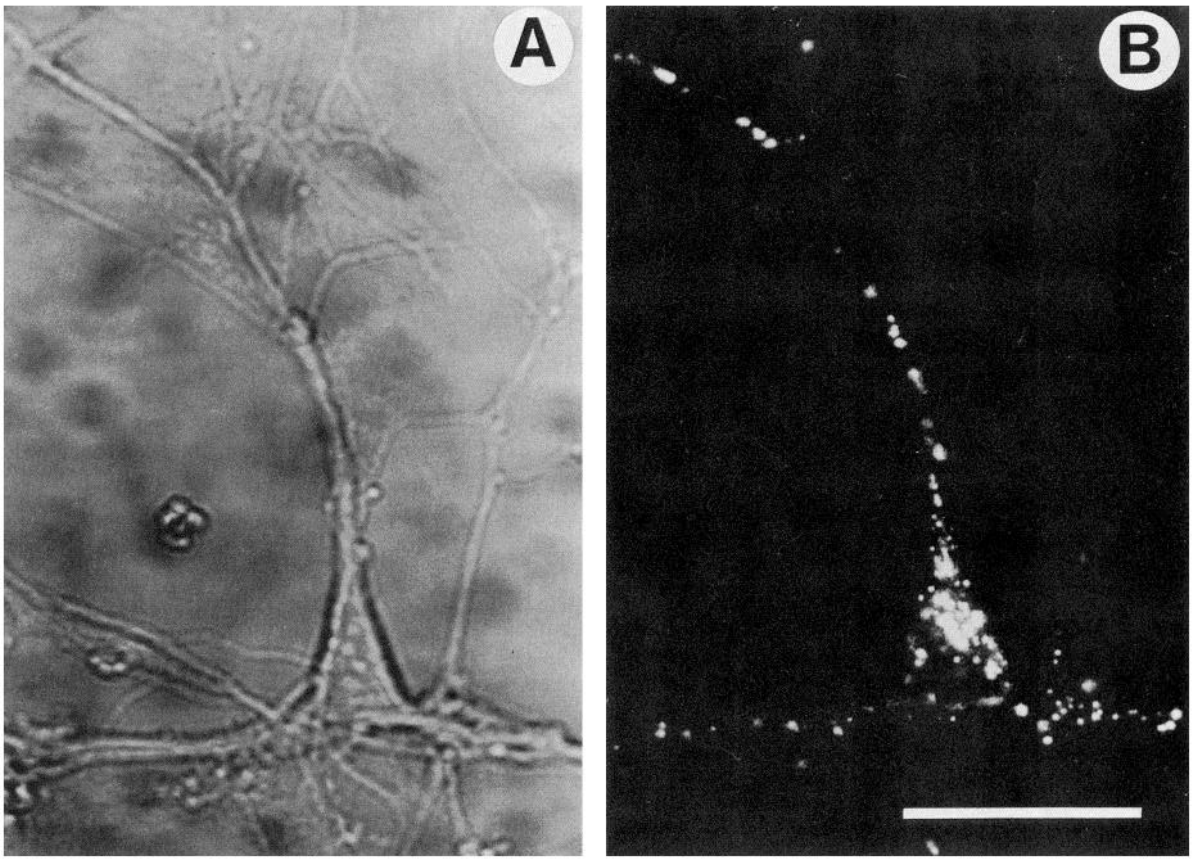

Figure 4. Distribution of M_1AChRs on rat visual cortical neurons in culture. A confocal image of a living cultured pyramidal neuron from rat visual cortex at 10 d *in vitro* (DIV) shows many M_1AChR binding sites labeled with BODIPY® FL PZ. Receptor binding sites are visualized both on the cell body and on the proximal portion of the dendrites (*B*). A same-field picture shows the neuron in phase contrast (*A*). Scale bar, 10 μm.

rons after only 24 hr in culture, although the receptor binding sites were sparse. Most of the visualized binding sites were localized in the area of the cell body from which the processes were growing out. There were also a few receptors distributed on the initial segments of processes. Figure 6*B* presents a comparable image of a representative neuron after 10 d in culture. The number of the fluorescent spots on the cell body were greatly increased at this stage and were also seen on the proximal portions of the dendrites. When visualized at day 17 (Fig. 6*C*), both the cell body and neuronal processes were heavily decorated with fluorescent "hot spots." The dendrites could be followed in favorable preparations over at least two branching points for distances as far as 600 μm.

Effect of membrane depolarization on development and expression of M_1 receptors

The binding of BODIPY® FL PZ to receptors on cultured visual cortical neurons increased significantly compared to control cultures after 7 d of treatment with 40 mM potassium chloride. Short periods of incubation of the cortical neurons with the KCl (1 or 2 d) had no obvious effect. This indicates that chronic depolarization of the neuronal membrane is necessary to upregulate the expression of M_1AChRs in these neurons. Pyramidal neurons of 17 DIV treated with 40 mM KCl during the final 7 d of incubation showed an increased number of fluorescent "hot spots" both on the cell bodies and on processes. It was not unusual to see the fluorescent spots lined up along extended

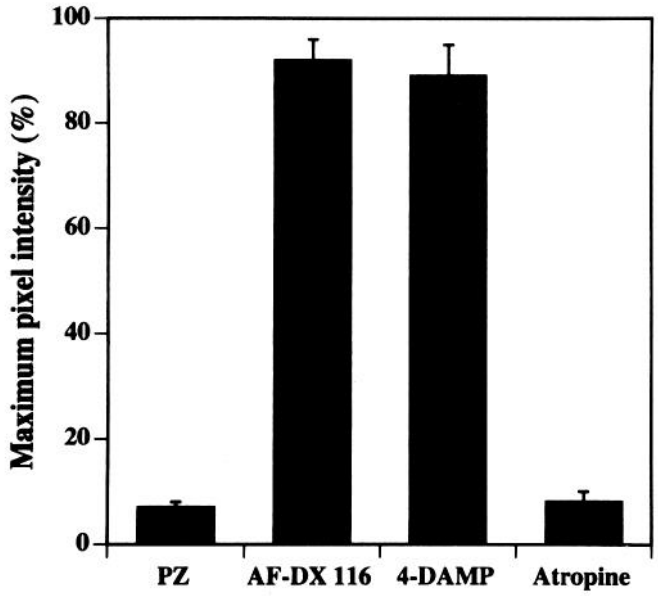

Figure 5. Competition of BODIPY® FL PZ binding with PZ, AF-DX 116, 4-DAMP, and atropine. Experimental details are as described in Materials and Methods. Values are the means (±SEM) of five experiments. Note that binding in the presence of unlabeled PZ and atropine is reduced to less than 10% of control values. AF-DX 116 and 4-DAMP have little effect on binding density.

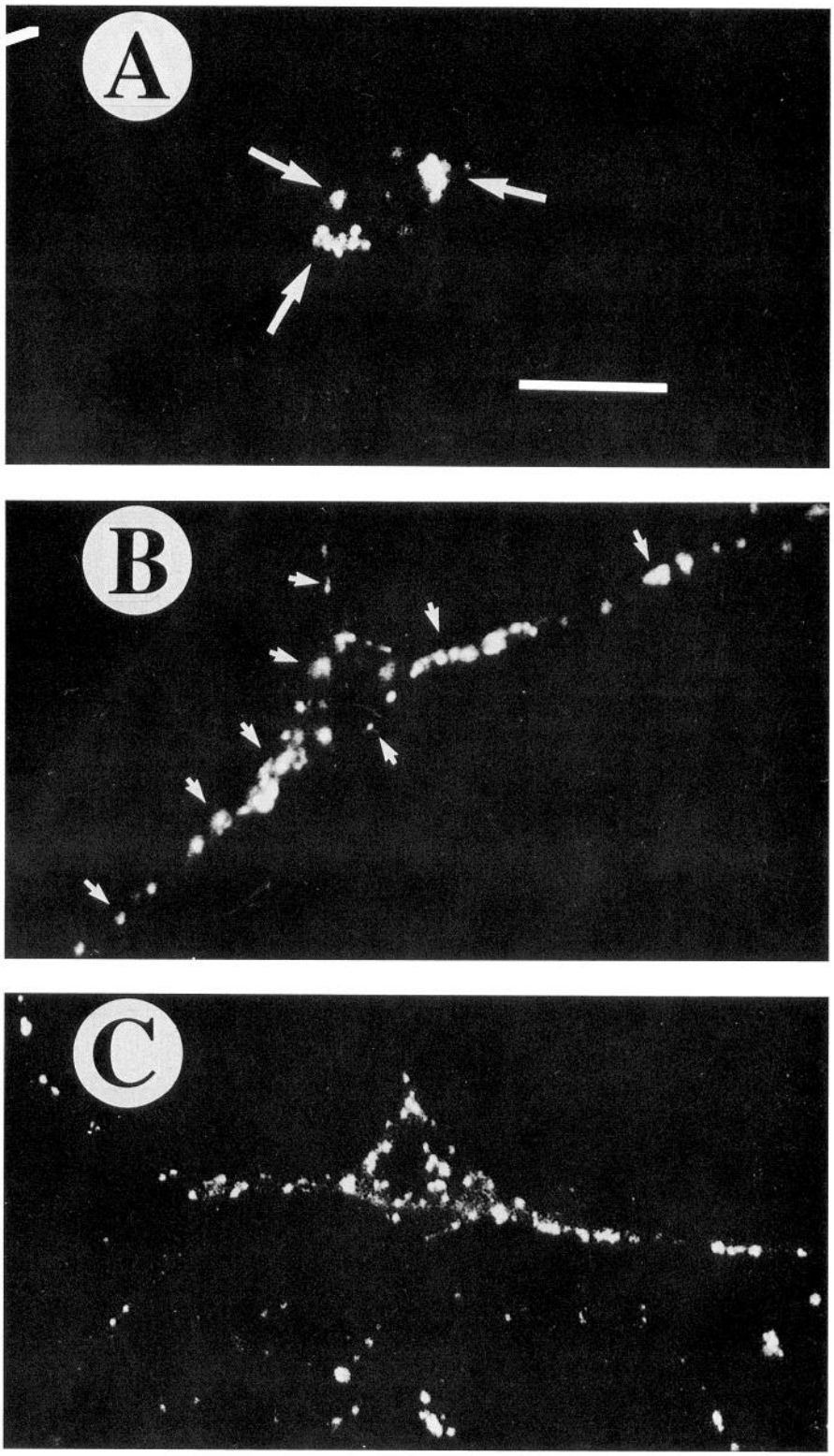

Figure 6. Developmental increase in the expression of M_1 receptor binding sites on rat visual cortical neurons in primary cell culture. Each panel (*A–C*) contains a confocal image of a representative cultured neuron labeled with fluorescent BODIPY® FL PZ. *A*, A neuron at 1 DIV expressing the receptor binding sites on its cell body and the initial segments of processes (*arrows*). *B*, By 10 DIV, the number of the fluorescent spots on neuronal cell bodies was greatly increased and they were also distributed on the proximal portion of the dendrites (*arrows*). *C*, A neuron at 17 DIV showing both cell body and processes enriched with fluorescently labeled M_1 receptors. Scale bar, 10 μm.

neuronal processes in these treated cultures. The cell illustrated in Figure 7*A* was cultured in a medium containing 40 mM potassium chloride for 7 d after 10 d of control culture conditions. Note the dramatic upregulation of fluorescently labeled M_1 receptors in the cell body of this neuron. Neurons with this enormous concentration of somatic binding sites were never observed in control cultures. Figure 8 shows the results of quantitative estimations of the receptor expression in the plasma membrane of cell bodies and processes from potassium-and TTX-treated as well as control cultures. In these quantitative estimations, the fluorescent spots per cell body and fluorescent spots per primary process followed as far as 100 μm from initial

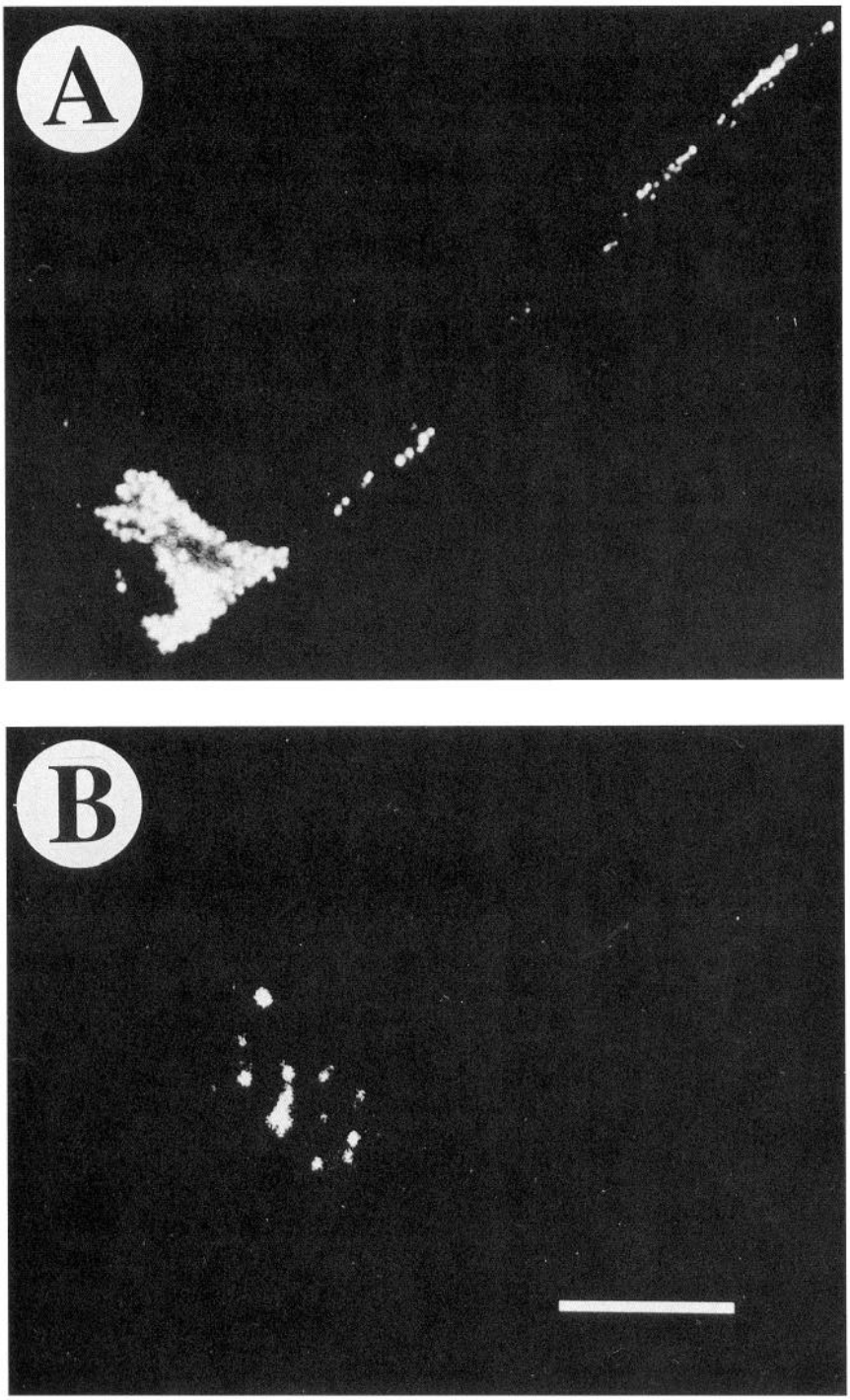

Figure 7. Confocal images of fluorescently labeled M_1 receptor binding sites in cultured visual cortical neurons treated with high K^+ or TTX. *A*, A typical 17 DIV neuron exposed to 40 mM KCl during the final 7 d of incubation. The receptor binding sites, shown as fluorescent "hot spots" show a high concentration on the cell body and processes. *B*, A representative neuron of the same age in a sister culture exposed to 0.1 μM TTX during the final 7 d of incubation. The number of receptor binding sites on this neuron is much less than in control neuron (see Fig. 6*C*). Scale bar, 20 μm.

exit point were counted from randomly chosen, independent profiles. The average numbers of fluorescent hot spots ± SEM per cell body and per process for each group were also calculated, and the percentage increase in number of "hot spots" relative to control is plotted in Figure 8. For high K^+–treated cultures, the number of fluorescent hot spots in the processes was found to be increased by 58% relative to control cultures (Fig. 8, bottom) and it was increased by about 40% in the cell bodies (Fig. 8, top). It should be noted, however, that the morphological appearance (e.g., the size and intensity) of individual "hot spots" in both high K^+–treated and untreated cultures was similar.

Effect of blocking bioelectric activity on expression of M_1 receptor binding sites

Using the methods as described in previous sections, the binding of BODIPY® FL PZ to cultured visual cortical neurons was studied in those cultures treated with TTX. In this experiment, 10-d-old cultured neurons were exposed to 0.1 μM TTX for another 7 d. As illustrated in Figure 7*B*, growing the cultures in the presence of TTX, which abolishes neuronal activity, causes a dramatic decrease in density of the receptors, especially on dendrites. Quantitative estimates showed that treatment of the

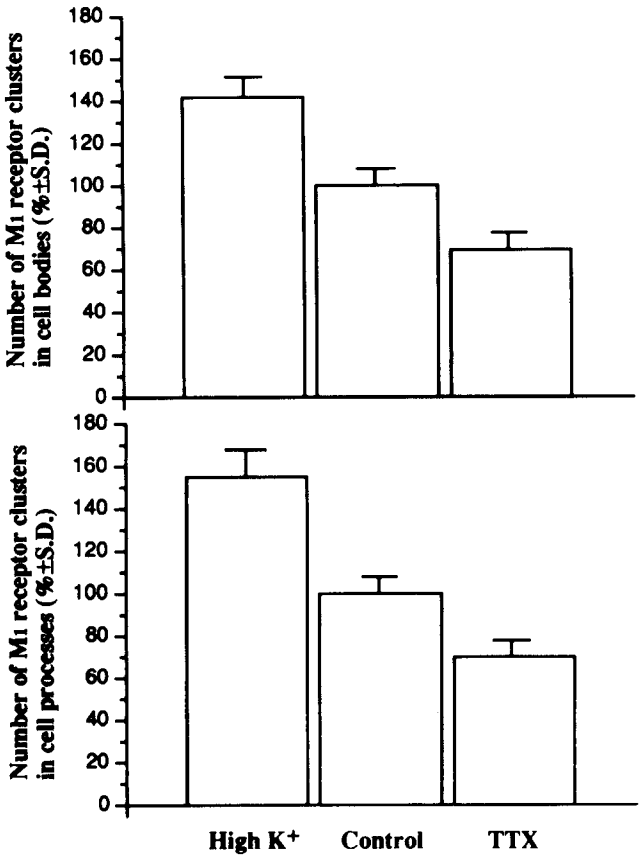

Figure 8. Effects of high concentration of potassium chloride and TTX on the expression of M_1 receptor in cultured visual cortical neuron. Results are presented as percentage increase or decrease in the number of M_1 receptor clusters relative to control values. Each value is the mean ± SEM of 18–30 determinations. *Top*, Number of the receptor clusters in cell bodies. *Bottom*, Number of the receptor clusters in cell processes.

neurons with 0.1 μM TTX for 7 d significantly decreased the number of fluorescent "hot spots" on both cell bodies and processes when compared with untreated control cultures (Fig. 8, bottom). As shown in Figure 8 the number of fluorescent "hot spots" in the processes was found to be decreased by 42% relative to control cultures and it was decreased by about 30% in the cell bodies. The effect appears to require chronic TTX treatment since it was not observed when the cultures were examined 1 or 2 d after TTX incubation. Despite the change in numbers, the size and fluorescent intensity of individual "hot spots" were not changed after TTX treatment.

Effect of chronic treatment with receptor agonists and antagonists

The classical M_1 receptor antagonist PZ and the muscarinic receptor agonist carbachol were used to treat the neuronal cultures during the period of cell growth to examine the up- or downregulating effect, if any, of chronic treatment with these agents on developmental expression of the M_1 receptor. The procedures were similar to those described above for treatment with TTX and high potassium concentration: 10-d-old cultured neurons were coincubated either with 10 μM carbachol or 5 nM PZ in the medium for another 7 d. As illustrated in Figure 9*A*, the number of receptor binding sites on cytoplasmic membranes of the neurons increased significantly after 7 d of incubation with 5 nM PZ when compared with the untreated control neurons. On the other hand, neurons treated with 10 μM carbachol for 7 d were characterized by a significant decrease in the number of receptor binding sites (Fig. 9*B*). Table 1 shows the results of quantitative estimations.

Discussion

We have developed a fluorescent analog, BODIPY® FL PZ, to study both activity-dependent and use-dependent expression of M_1AChRs on cultured visual cortical neurons. As the results from the competitive binding assays show, the fluorescent PZ derivative used here retained its affinity to M_1AChRs and was a potent inhibitor of ^{3}H-PZ binding to rat brain cortex membrane just as was native PZ. Likewise, the displacement profile of BODIPY® FL PZ was similar to native PZ. The high affinity and well-characterized specificity of BODIPY® FL PZ for the M_1 receptor shown in our results, make this as an ideal ligand to study the dynamics of M_1 receptor behavior by fluorescent imaging with confocal microscopy. It is clear that the high-resolution confocal laser scanning microscope has several advantages over standard epifluorescence optics. These include both increased sensitivity and spatial resolution as well as reduced bleaching of fluorochrome due to the serial scanning method by which the image is formed. In addition, the ability to scan the specimen optically through various depths at specific intervals and then to composite the image data to form an extended-focus image of the object of interest is a powerful

Table 1. Quantification of M_1 receptor clusters expressed as fluorescent hot spots in the plasma membrane of cultured rat visual cortical neurons treated with PZ or carbachol

	Treatment		
Location	PZ	Carbachol	Control
Cell bodies	22.8 ± 2.4 (n = 20)*	9.1 ± 1.2 (n = 20)*	16.6 ± 1.0 (n = 25)
Processes	11.5 ± 0.6 (n = 20)**	3.2 ± 0.5 (n = 20)**	6.4 ± 0.5 (n = 19)

Data are quantification of the expression of M_1 receptor binding sites in the plasma membrane of cell bodies and processes from receptor agonist- and antagonist-treated and untreated control cultures of rat visual cortical neurons. Visual cortical neurons were cultured for 17 d and subsequently prepared for confocal visualization of M_1 receptors as described in the text. During the last 7 d of culture the agonist-treated cultures were grown in the presence of 10 μM carbachol and the antagonist-treated cultures were grown in the presence of 5 nM PZ. The average numbers of fluorescent hot spots ± SEM per cell body and per process are based on counting of 20 randomly chosen, independent profiles.

* Significantly different ($P < 0.01$) from the number of M_1 receptor clusters on the cell bodies of control group (Student's paired t test).

** Significantly different ($P < 0.01$) from the number of M_1 receptor clusters on the cell processes of control group (Student's paired t test).

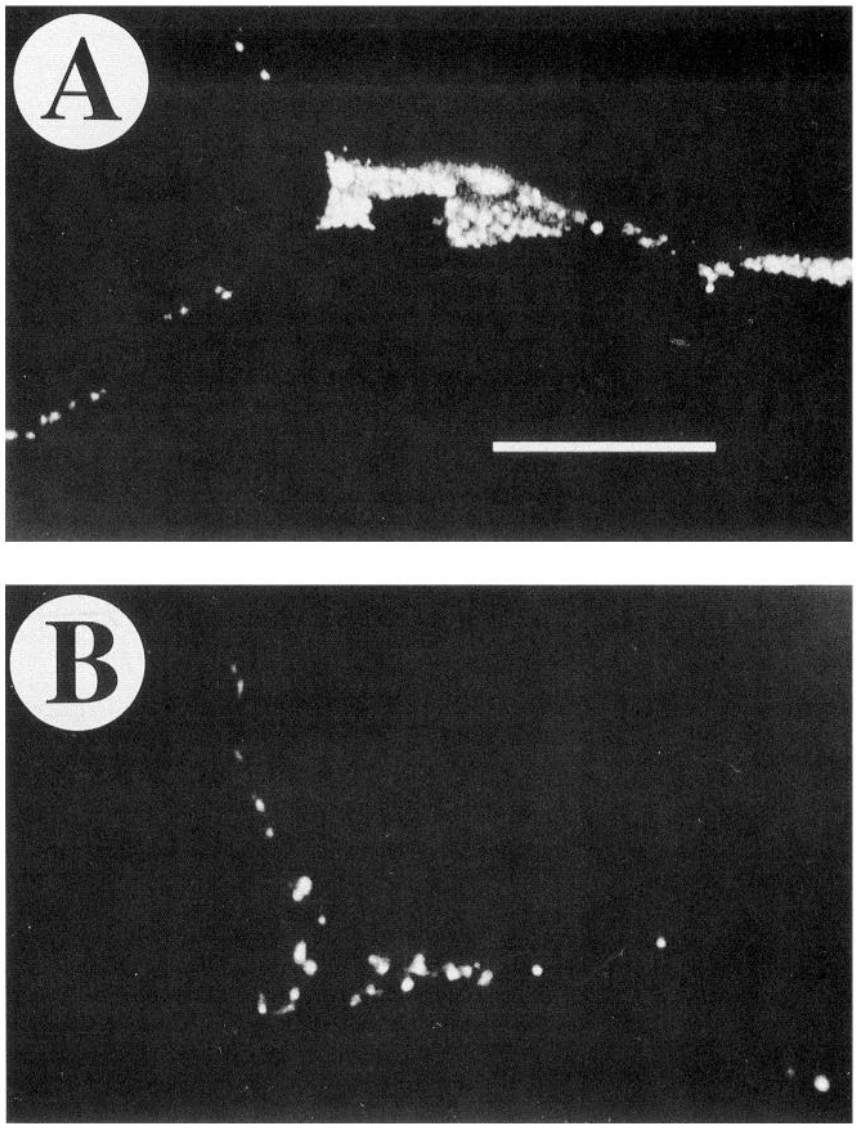

Figure 9. Confocal imaging of fluorescently labeled M_1 receptor binding sites in cultured visual cortical neurons treated with the receptor agonist charbacol and antagonist PZ. *A*, A representative 17 DIV neuron treated with 5 nM PZ during the final 7 d of incubation showed a great increase of receptor binding sites. *B*, A representative 17 DIV neuron of the same age in a sister culture treated with 10 mM carbachol during final 7 d of incubation showed the opposite result. Scale bar, 10 μm.

advantage. The results presented in this article are therefore considered to be rather reliable, particularly the qualitative and quantitative procedures for measuring density and distribution of receptor binding sites.

Developmental expression of M_1 receptors in normal cultures

In normal nontreated cultures, as indicated in the Results, the receptors were present only at very low levels at postnatal day 0 immediately after dissociation. They then gradually increased in number over the next 2–3 weeks. At early ages (the first week in culture), the receptors started to appear on the initial segments of the axonic and dendritic outgrowths and redistributed within somata to form zone of high M_1 concentration. In the second week in culture, the receptors were not only apparent on cell bodies and initial segments of the cell extensions, but were also expressed at a distance in secondary and tertiary branches of the extensions, forming several high-density "hot spots." This expression shift might reflect the formation of synaptic contacts and/or transmission at this stage. During the last stage (the third week in the culture), the receptor binding sites were imaged almost everywhere on the somal surface as well as in visible branches, which correlates with the peak of synaptic development and its stabilization in culture at this stage. The neuronal extensions, including axons and dendrites, began to retract after 3 weeks in culture, as has been observed previously in rat cerebral cortex neurons (Ramakers et al., 1991), and the number of receptors decreased following the somatal and neuritic degeneration. This neuron death after 3 weeks in culture condition may be caused by the lack of contact with an appropriate neuronal target (Innocenti et al., 1977; Cowan and O'Leary, 1984).

Glial cells were identifiable in these cultures on morphological grounds, and we were interested to find evidence of muscarinic receptor localization on these cells as well. The rules underlying receptor regulation on glial cells will be the subject of a separate communication.

The expression and distribution of M_1 receptors have been studied at the whole-animal level in the developing cat (Prusky and Cynader, 1990) and rat (unpublished observations) in previous autoradiographic studies in our laboratory. These findings indicated that M_1 receptors were expressed in layer IV immediately following birth. The density of the receptors increased at different rates in the different cortical layers to achieve a

relatively homogeneous distribution across all cortical layers at 30–40 d of age with a later concentration in the superficial and deep layers of the cortex. While we must be cautious in extrapolating results from these culture experiments to the *in vivo* situation, the results reported here show that a similar gradual increase in M_1AChR number occurs on both cell bodies and neuronal processes in the culture environment from day 0 to day 21.

Effect of chronic high potassium and TTX treatment on M_1 receptor expression

A primary finding reported here is the elucidation of some factors that regulate the expression and distribution of M_1AChR during development. The results obtained here are quite clear in showing that the number of M_1 receptors was increased by depolarization with chronic exposure to high concentrations of potassium chloride and decreased by blocking activity with chronic exposure to TTX.

Spontaneously occurring bioelectric activity has been shown to be a significant factor in neuronal development, affecting both morphological and functional aspects of the nervous system (Harris, 1981; Oppenheim, 1985; for review, see Fields and Nelson, 1992). In kitten visual cortex, it has been found that the expression and redistribution of neurotransmitter receptors observed during the critical period are also dependent on visual input to the cortex (Cynader et al., 1990). In the present study we found that chronic depolarization by high concentration of potassium or chronic blocking of activity by TTX was necessary to modulate M_1 receptor expression. Similar chronic responses have been induced by high potassium treatment in the study of muscarinic receptors in septal neurons (Simantov and Levy, 1989). In the study of synaptogenesis in rat cerebral cortex cultures using quantitative stereological EM analysis (Van Huizen et al., 1985), it was revealed a significant retardation in synapse formation and ultrastructural maturation of synaptic junctions occurred during the first 3 weeks in culture when the occipital cortex cells were chronically exposed to impulse-blocking levels of TTX. Chronic suppression of spontaneously occurring bioelectric activity by TTX was also reported to induce cellular biochemical changes and increase neuronal cell death in cerebral cortex cultures (Ramakers and Boer, 1991; Ramakers et al., 1991). However, the molecular mechanisms underlying the effect of chronic activation or suppression of bioelectric activity on the development of axonal and dendritic form and receptor expression are not yet clear. A number of possible cellular and molecular mechanisms involved in these chronic processes have been considered. First of all, the effect of neural electric activity directly modulates membrane potential, which could (1) change the level of trophic materials, such as NGFs, released by neurons and glial cells (Gall and Isackson, 1989); (2) modulate voltage-dependent ion channels (Simantov and Levy, 1989) to affect the formation of neuronal processes and the expression of neurotransmitter receptors. A number of substances, such as arachidonic acid and nitric oxide, released by the postsynaptic neuron in response to depolarization have also been suggested as having possible postsynaptic effects (for review, see Fields and Nelson, 1992). In addition, electrical activity has been shown to modulate intracellular calcium and a number of second messenger systems, which may affect the development of axonal and dendritic form and the expression of neurotransmitter receptors. For instance, elevated intracellular calcium may activate a protease that increases the number of glutamate receptors (Lynch and Baudry, 1984). Finally, in addition to modulation of the level of trophic factors and calcium, electrical activity has been shown to produce changes in a number of regulatory genes such as c-fos (Morgan and Curran, 1989) and Zif-268 (Chaudhuri and Cynader, 1993).

Effect of cholinergic input on M_1 receptor expression

Our results reveal that the expression of M_1AChRs depends not only on neuronal activity, but also on the occupancy of the existing M_1AChR. Chronic application of the mAChR agonist carbachol for 7 d in culture condition decreased the density of fluorescent binding sites, while M_1AChR antagonist PZ increased fluorescent binding sites.

The chronic process of antagonist-induced upregulation of mAChRs has also been investigated in other neuronal preparations (Niu et al., 1989; Vige and Briley, 1989; Ohkuma et al., 1990). Previous work has shown that the muscarinic receptor antagonists atropine (1 μM) and PZ (10 μM) cause a significant upregulation of mAChR mRNA. Increase in M_1 receptor mRNA was also found in temporal cortex of Alzheimer's disease patients, as demonstrated by *in situ* hybridization histochemistry (Harrison et al., 1991). Therefore, elevated levels of muscarinic receptor mRNA are likely to result in increased receptor synthesis in response to antagonist inhibition and to the cholinergic deficits occurring in Alzheimer disease. On the other hand, it has been shown that short-term exposure of mAChRs to ACh or to its analog carbachol causes losses of function (desensitization) of muscarinic receptors. Agonist application apparently induces internalization of surface mAChRs, which is not necessarily associated with a significant change in the total number of cellular receptors (Ray et al., 1989). Prolonged exposure of mAChR to either ACh or carbachol leads to gradual decrease in the concentration of these receptors due to an increased rate of mAChR degradation (Klein et al., 1979). Electron microscopic immunocytochemistry, using a monoclonal anti-muscarinic receptor antibody, has revealed that the mAChR downregulation may be brought about by internalization of the receptor into intracellular vesicles (Rapaso et al., 1987). More recent work using specific binding assay and Northern blot hybridization analysis to evaluate the levels of M_1AChRs and their mRNA levels in a transfected cell line suggests that the reduction in steady state level of muscarinic receptors following prolonged treatment with agonist is not solely the result of an increase in the rate of receptor degradation, but could also result from a decrease in receptor protein synthesis as a consequence of a decrease in the level of its mRNA (Wang et al., 1990). Similar results have been reported for M_2 and M_3 muscarinic ACh receptors in cultured cerebellar granule cells (Fukamauchi et al., 1991).

Another factor regulating mAChRs in rat cerebral cortical slices appears to involve second messenger systems. Jia et al. (1989) showed that activation of protein kinase C with phorbol esters caused marked downregulation of mAChR. They suggested a feedback pathway in which phosphatidylinositol turnover elicited by stimulation of mAChRs, which results in protein kinase C activation, is involved in the receptor downregulation. This evidence suggests that activation of other noncholinergic receptors coupled to phosphatidylinositol turnover might also downregulate mAChRs. As new fluorescent ligands for various receptors become available, the ability to visualize their exact spatial relationships to each other will be an important advantage in studies of regulatory mechanisms.

In conclusion, our results indicate that the developmental expression of M_1 receptors is regulated by neuronal activity and also by occupancy of the receptor. Whether one of the above factors plays a dominant role in regulating receptor expression, and whether there are interaction between them is an important issue for future study.

References

Araujo DM, Lapchak PA, Quirion R (1991) Heterogeneous binding of [^{3}H]4-DAMP to muscarinic cholinergic sites in the rat brain: evidence from membrane binding and autoradiographic studies. Synapse 9:165–176.

Bear MF, Singer W (1986) Modulation of visual cortical plasticity by acetylcholine and noradrenaline. Nature 320:172–176.

Beaulieu C, Cynader M (1990a) Effect of the richness of the environment on neurons in cat visual cortex. I. Receptive field properties. Dev Brain Res 53:71–81.

Beaulieu C, Cynader M (1990b) Effect of the richness of the environment on neurons in cat visual cortex. II. Spatial and temporal frequency characteristics. Dev Brain Res 53:82–88.

Bhattacharya SK, Sen AP, Das-Gupta G, Seth K, Seth PK (1991) Central muscarinic receptor subtypes and carrageenin-induced paw edema in rats. Res Exp Med 191:65–76.

Birdsall N, Burgen A, Hulme EC (1978) The binding of agonists to brain muscarinic receptors. Mol Pharmacol 14:723–736.

Brown DA, Foreward A, Marsh J (1980) Antagonist discrimination between ganglionic and ileal muscarinic receptors. Br J Pharmacol 71:362–364.

Brown DA, Foreward A, Marsh J (1987) Antagonist discrimination between ganglionic and ideal muscarinic receptors. Br J Pharmacol 71:362–364.

Carlsson K, Aslund N (1987) Confocal imaging for 3-digital microscopy. Appl Opt 26:3232–3238.

Carlsson K, Wallen P, Brodin L (1989) Three-dimensional imaging of neurons by confocal fluorescence microscopy. J Microscopy 155: 15–26.

Chaudhuri A, Cynader MS (1993) Activity-dependent expression of the transcription factor Zif268 reveals ocular dominance columns in monkey visual cortex. Brain Res 605:349–353.

Cheng YC, Prusoff WH (1973) Relationship between inhibition constant (K_i) and the concentration of inhibitor which causes 50% inhibition (I_{50}) of an enzymatic reaction. Biochem Pharmacol 22:3099–3108.

Cowan WM, O'Leary DDM (1984) Cell death and process elimination: the role of regressive phenomena in the development of the vertebrate nervous system. In: Medicine, science and society (Isselbacher KJ, ed), pp 643–668. New York: Wiley.

Cynader M, Shaw C, van Huizen F, Prusky G (1990) Transient receptor expression in visual cortex development and the mechanisms of cortical plasticity. In: The neocortex (Finlay BL, et al., eds), pp 245–253.

El-Fakahany EE, Lee JH (1986) Agonist-induced muscarinic acetylcholine receptor down-regulation in intact rat brain cells. Eur J Pharmacol 132:21–30.

Fields RD, Nelson PG (1992) Activity-dependent development of the vertebrate nervous system. Int Rev Neurobiol 34:133–213.

Fukamauchi F, Hough C, Chuang DM (1991) Expression and agonist-induced down-regulation of mRNAs of M2 and M3-muscarinic acetylcholine receptors in cultured cerebellar granule cells. J Neurochem 56:716–719.

Gabridge MG (1981) The chamber/dish: an improved vessel for cell and explant culture. In Vitro 17:91–97.

Giraldo E, Monferini E, Hanner R (1985) Selective labeling of M1 receptors in autonomic ganglia with (3)H-pirenzepine. Drug Res 35: 325–328.

Greene LA, Rein G (1976) Synthesis, storage and release of acetylcholine by as noradrenergic pheochromocytoma cell line. Nature 268: 349–351.

Gu Q, Singer W (1993) Effects of intracortical infusion of anticholinergic drugs on neuronal plasticity in kitten striate cortex. Eur J Neurosci 5:475–485.

Hammer R, Berrie CP, Birdsall N, Burgen A, Hulme EC (1980) Pirenzepine distinguishes between different subclasses of muscarinic receptors. Nature 283:90–92.

Harris WA (1981) Neural activity and development. Annu Rev Physiol 43:689–710.

Harrison PJ, Barton AJL, Najlerahim A, McDonald B, Pearson RCA (1991) Increased muscarinic receptor messenger RNA in Alzheimer's disease temporal cortex demonstrated by *in situ* hybridization histochemistry. Mol Brain Res 9:15–21.

Hulme EC, Birdsall NJM, Buckley NJ (1990) Muscarinic receptor subtypes. Annu Rev Pharmacol Toxicol 30:633–673.

Hunter DD, Nathanson NM (1986) Biochemical and physical analysis of newly synthesized muscarinic acetylcholine receptors on cultured embryonic chicken cardiac cells. J Neurosci 6:3739–3784.

Innocenti GM, Fiore L, Caminiti R (1977) Exuberant projections into the corpus callosum from the visual cortex of newborn cats. Neurosci Lett 4:237–242.

Jia WG, Shaw C, Van Huizen, Cynader MS (1989) Phorbol 12,13-dibutyrate regulates muscarinic receptors in rat cerebral cortical slices by activating protein kinase C. Mol Brain Res 5:311–315.

Karton Y, Bradbury BJ, Baumgold J, Paek R, Jacobson KA (1991) Functionalized congener approach to muscarinic antagonists: analogues of pirenzepine. J Med Chem 34:2133–2145.

Klein WL, Nathanson N, Nirenberg M (1979) Muscarinic acetylcholine receptor regulation by accelerated rate of receptor loss. Biochem Biophys Res Commun 90:506–512.

Lynch G, Baudry M (1984) The biochemistry of memory: a new and specific hypothesis. Science 224:1057–1063.

Maloteaux J, Gossuin A, Pauwels PJ, Laduron PM (1983) Short-term disappearance of muscarinic cell surface receptors in carbachol-induced desensitization. FEBS Lett 156:103–107.

Martinez F, Bali JP, Rodriguez M, Castro B, Magous R, Laur J, Lignon MF (1985) Synthesis and biological activities of some pseudo-peptide analogues of tetragastrin: the importance of the peptide backbone. J Med Chem 28:1874–1879.

Mash DC, Potter LT (1986) Autoradiographic localization of M1 and M2 muscarine receptors in the rat brain. Neuroscience 19:551–654.

Morgan JI, Curran T (1989) Calcium and proto-oncogene involvement in the immediate-early response in the nervous system. Ann NY Acad Sci 568:283–290.

Niu WZ, Zhao DL, Liu CG (1989) Up-regulation of muscarinic receptor of canine cerebral cortex by chronic treatment of a new anticholinergic drug. Chin J Pharmacol Toxicol 3:196.

Ohkuma S, Kishi M, Ma FH, Kuriyama K (1990) Alterations in receptor-coupled second messenger systems at up-regulated muscarinic receptors: analysis using primary cultured neurons. Eur J Pharmacol Mol Pharmacol 189:277–285.

Oppenheim RW (1985) Naturally occurring cell death during neural development. Trends Neurosci 8:487–493.

Pawley JB (1991) Fundamental and practical limits in confocal light microscopy. Scanning 13:184–198.

Pedigo NW Jr (1988) Pharmacological adaptations and muscarinic receptor plasticity in hypothalamus of senescent rats treated chronically with cholinergic drugs. Psychopharmacology 95:497–501.

Pilch H, Muller WE (1988) Chronic treatment with choline or scopolamine indicates the presence of muscarinic cholinergic receptor plasticity in the frontal cortex of young but not of aged mice. J Neural Transm 71:39–43.

Prusky G, Cynader M (1990) The distribution of M1 and M2 muscarinic acetylcholine receptor subtypes in the developing cat visual cortex. Dev Brain Res 56:1–12.

Ramakers GJA, Boer GJ (1991) Chronic suppression of bioelectric activity and cell survival in primary cultures of rat cerebral cortex: biochemical observations. Eur J Neurosci 3:154–161.

Ramakers GJA, Raadsheer FC, Corner MA, Ramaekers FCS, van Leeuwen FW (1991) Development of neurons and glial cells in cerebral cortex, cultured in the presence or absence of bioelectric activity: morphological observations. Eur J Neurosci 3:140–153.

Rapaso G, Dunia I, Marullo S, Andre C, Guillet JG, Strosberg AD, Benedetti EL, Hoebeke J (1987) Redistribution of muscarinic acetylcholine receptors on human fibroblasts indicated by regulatory ligands. Biol Cell 60:117–124.

Ray P, Middleton W, Berman JD (1989) Mechanism of agonist-induced down-regulation and subsequent recovery of muscarinic acetylcholine receptors in a clonal neuroblastoma × fliona hybrid cell line. J Neurochem 52:402–409.

Rimvall K, Keller F, Waser PG (1989) Muscarinic receptors on cultured cells of rat hippocampus: cholinergic regulation and presence of subtypes. Eur J Pharmacol 160:1–9.

Shaw C, Van Huizen F, Cynader MS, Wilkinson M (1989) A role for potassium channels in the regulation of cortical muscarinic acetylcholine receptors in an *in vitro* slice preparation. Brain Res 5:71–83.

Shotton DM (1989) Confocal scanning optical microscopy and its applications for biological specimens. J Cell Science 94:175–206.

Sillito AM, Kemp JA (1983) Cholinergic modulation of the functional organization of the cat visual cortex. Brain Res 289:142–155.

Simantov R, Levy R (1989) Selective regulation of different muscarinic receptors in septum and hippocampus neuronal cultures. Brain Res 505:160–162.

Singer W (1979) Central-core control of visual cortex functions. In: The neurosciences, Fourth study program (Schmitt FO, Worden FG, eds), pp 1093–1110. Cambridge, MA: MIT Press.

Spencer DG, Horvath E, Traber J (1986) Direct autoradiographic determination of M1 and M2 muscarinic acetylcholine receptor distribution in the rat brain: relation to choline receptor distribution in the rat brain: relation to cholinergic nuclei and projections. Brain Res 380:59–68.

Thompson AK, Fisher SK (1990) Relationship between agonist-induced muscarinic receptor loss and desensitization of stimulated phosphoinositide turnover in two neuroblastomas: methodological considerations. J Pharmacol Exp Ther 252:744–752.

Triller A, Seitanidou T, Franksson O, Korn H (1991) Use of confocal microscope for the cellular analysis of the glycine synaptic receptor. J Receptor Res 11:347–357.

Van Huizen F, Romijn HJ, Habets AMMC (1985) Synaptogenesis in rat cerebral cortex cultures is affected during chronic blockade of spontaneous bioelectric activity by tetrodotoxin. Dev Brain Res 19: 67–80.

Van Huizen F, Romijn HJ, Habets AMMC, van den Hooff P (1987) Accelerated neural network formation in rat cerebral cortex cultures chronically disinherited with picrotoxin. Exp Neurol 97:280–288.

Van Huizen F, Shaw C, Wilkinson M, Cynader M (1989) Characterization of muscarinic acetylcholine receptors in rat cerebral cortex slices with concomitant morphological and physiological assessment of tissue viability. Mol Brain Res 5:59–69.

Vige X, Briley M (1989) Muscarinic receptor plasticity in rats lesioned in the nucleus basalis of Meynert. Neuropharmacology 28:727–732.

Vincent SL, Sorensen I, Benes FM (1991) Localization and high-resolution imaging of cortical neurotransmitter compartments using confocal laser scanning microscopy: GABA and glutamate interactions in rat cortex. Biotechniques 11:628–634.

Wang SZ, Hu J, Long RM, Pou WS, Forray C, El-Fakahany EE (1990) Agonist-induced down-regulation of m1 muscarinic receptors and reduction of their mRNA level in a transfected cell line. FEBS Lett 276:185–188.

Watson M, Roeske WR, Yamamura HI (1982) [^{3}H]-pirenzepine selectively identifies a high affinity population of muscarinic cholinergic receptors in the rat cerebral cortex. Life Sci 31:2019–2023.

Zhu XE, Chuang DM (1988) Differential regulation by butyrate and dibutyryl cyclic AMP of delta-opioid, alpha-2-adrenergic, and muscarinic cholinergic receptors in NCB-20 cells. J Neurochem 50:17–26.